REPORT DOCUMENTATION PAGE

Form Approved
OMB No. 0704-0188

1. REPORT DATE *(DD-MM-YYYY)*	**2. REPORT TYPE**	**3. DATES COVERED** *(From - To)*
19-06-2008	Technical Paper	

4. TITLE AND SUBTITLE

Assessment of Translational Anisotropy in Rarefied Flows Using Kinetic Approaches (Preprint)

5a. CONTRACT NUMBER

5b. GRANT NUMBER

5c. PROGRAM ELEMENT NUMBER

6. AUTHOR(S)
D.C. Wadsworth & N.E. Gimelshein (ERC); S.F. Gimelshein (USC); I.J. Wysong (AFRL/RZSA)

5d. PROJECT NUMBER

5e. TASK NUMBER
23080532

5f. WORK UNIT NUMBER

7. PERFORMING ORGANIZATION NAME(S) AND ADDRESS(ES)

Air Force Research Laboratory (AFMC)
AFRL/RZSA
10 E. Saturn Blvd.
Edwards AFB CA 93524-7680

8. PERFORMING ORGANIZATION REPORT NUMBER

AFRL-RZ-ED-TP-2008-252

9. SPONSORING / MONITORING AGENCY NAME(S) AND ADDRESS(ES)

Air Force Research Laboratory (AFMC)
AFRL/RZS
5 Pollux Drive
Edwards AFB CA 93524-7048

10. SPONSOR/MONITOR'S ACRONYM(S)

11. SPONSOR/MONITOR'S NUMBER(S)
AFRL-RZ-ED-TP-2008-252

12. DISTRIBUTION / AVAILABILITY STATEMENT

Approved for public release; distribution unlimited (PA #08264A).

13. SUPPLEMENTARY NOTES
For presentation at the 26th International Symposium on Rarefied Gas Dynamics, Kyoto, Japan, 21-25 July 2008.

14. ABSTRACT

Several distinct modeling approaches are tested for their ability to resolve translational nonequilibrium phenomena that are common to (but not unique to) rarefied gas dynamic flowfields. The methods considered include DSMC, BGK, ES-BGK, Navier-Stokes, and an anisotropic model (based on a first order expansion of the Boltzmann equation for a Maxwell gas possessing an anisotropic Maxwellian distribution function). For the large Mach number normal shock wave, ES-BGK shows fair-to-good agreement with DSMC, while numerical solution of the anisotropic model equations are rather poor. A semi-analytical solution for the anisotropic model compares rather well with DSMC results for the normal shock wave, suggesting that the equation set may indeed be quantitatively useful for modeling translational nonequilibrium. For the hypersonic sphere-cone flowfield, comparison of the directly sampled shear stress with the Navier-Stokes (Chapman-Enskog) and anisotropic value evaluated using the DSMC macroscopic properties shows that the anisotropic result offers qualitative improvement over the NS value over a broad range of rarefaction.

15. SUBJECT TERMS

16. SECURITY CLASSIFICATION OF:			**17. LIMITATION OF ABSTRACT**	**18. NUMBER OF PAGES**	**19a. NAME OF RESPONSIBLE PERSON**
					Dr. Ingrid Wysong
a. REPORT	**b. ABSTRACT**	**c. THIS PAGE**	SAR	7	**19b. TELEPHONE NUMBER** *(include area code)*
Unclassified	**Unclassified**	**Unclassified**			N/A

Assessment of Translational Anisotropy in Rarefied Flows Using Kinetic Approaches (Preprint)

D. C. Wadsworth and N. E. Gimelshein*, S. F. Gimelshein† and I. J. Wysong**

*ERC, Inc., Edwards AFB, CA 93528
†University of Southern California, Los Angeles, CA 90089
**Propulsion Directorate, Edwards AFB, CA 93528

Abstract. Several distinct modeling approaches are tested for their ability to resolve translational nonequilibrium phenomena that are common to (but not unique to) rarefied gas dynamic flowfields. The methods considered include DSMC, BGK, ES-BGK, Navier-Stokes, and an anisotropic model (based on a first order expansion of the Boltzmann equation for a Maxwell gas possessing an anisotropic Maxwellian distribution function). For the large Mach number normal shock wave, ES-BGK shows fair-to-good agreement with DSMC, while numerical solution of the anisotropic model equations are rather poor. A semi-analytical solution for the anisotropic model compares rather well with DSMC results for the normal shock wave, suggesting that the equation set may indeed be quantitatively useful for modeling translational nonequilibrium. For the hypersonic sphere-cone flowfield, comparison of the directly sampled shear stress with the Navier-Stokes (Chapman-Enskog) and anisotropic value evaluated using the DSMC macroscopic properties shows that the anisotropic result offers qualitative improvement over the NS value over a broad range of rarefaction.

INTRODUCTION

Anisotropy of the molecular velocity distribution function is important for rarefied gases characterized by strong thermal non-equilibrium. Such a translational anisotropy arises both in compression flows dominated by shock waves, and expanding flows such as nozzle expansions and plumes. The need to account for the anisotropy in nonequilibrium gases was understood as early as 1867 [1]. Besides the transitional rarefied flow regime, this anisotropy may be important in turbulent flow modeling, especially when the transition to turbulence needs to be predicted. The latter one is traditionally approached with continuum methods based on the solution of Navier-Stokes equations, which, as was pointed out in [2], may not be the correct approximate solution of the Boltzmann equation for this case. In [2], an anisotropic fluid seven equation set was presented for the density, three fluid velocity components, and three directional thermal kinetic energies. This technique represents a macroscopic (20 moment) approach to non-equilibrium flows, and as such complements microscopic, kinetic methods, in their consideration of flow nonequilibrium. A semi-analytical solution to this equation set is also available [3] for the normal shock. In the past, several researchers have attempted to include translational non-equilibrium in a macroscopic fashion. Candler *et al.* [4] developed a multi-temperature equation set and compared numerical solutions for the normal shock wave problem with DSMC results. Dogra *et al.* [5] presented calculations using a multi-temperature model for unsteady blast-type problems. Baganoff [6] has presented a numerical method for Maxwell's moment equations for the normal shock problem.

The main objective of this work is an assessment of the accuracy of translational nonequilibrium predictions obtained with different approaches. In addition to [2] and [3], the following numerical methods are used: the direct simulation Monte Carlo method, that is considered to provide benchmark solutions; the finite volume solution of model kinetic equations, and the solution of Navier-Stokes equations as a reference point in comparing macroparameters. SMILE tool [7] was used for the DSMC computations, SMOKE solver recently developed at ERC provided the model kinetic equation capability, and the commercial Fluent [8] code was applied to obtain Navier-Stokes results.

The DSMC method is considered the most accurate approach for the present study, and indeed supplies the reference data by which the other methods are evaluated. A deterministic mathematical equation set, however, can offer benefits in, e.g., order of magnitude analysis, which can greatly assist in interpreting the physical phenomena involved. Two model problems are considered to assess nonequilibrium: the structure of a normal shock wave over the Mach number range $1.2 \leq M_\infty \leq 10$, and the hypersonic flow past a blunt sphere cone at moderate rarefaction $10^{-3} \leq Kn \leq 10^{-1}$.

NUMERICAL METHODS

DSMC

The 2D/axisymmetric capability of SMILE[7] was used for the DSMC computations. The majorant frequency scheme[9] was used to calculate intermolecular interactions. The intermolecular potential was assumed to be a variable hard sphere[10] with the value of $\omega = 0.5$ in the viscosity-temperature dependence in order to simulate the Maxwell molecule interaction used in all other methods applied in this work. For one-dimensional normal shock wave calculations, specular surfaces were used to provide a pseudo-1D setup. For 2D calculation of an external flow, fully diffuse reflection was assumed for gas-surface collisions. The total number of simulated molecules and collision cells for 1D runs was approximately 1 million and 1,000, respectively, and for 2D runs, 5 million and 1 million, respectively.

ES-BGK

A finite volume 2D/axisymmetric code SMOKE developed at ERC has been used to solve the BGK and ES-BGK equations. SMOKE is a parallel code based on conservative numerical schemes developed by L. Mieussens [11]. A second order spatial discretization is used along with implicit time integration. 1,000 spatial cells were used, with specular boundaries set to model 1D flow in the longitudinal direction. The convergence on the velocity grid was studied, with the number of (x,y,z) velocity points ranging from (30,20,20) to (60,40,40). The results for the latter one are presented below.

Navier-Stokes

Calculations are performed with a standard commercial CFD code, Fluent [8]. A density-based Navier-Stokes solution was obtained for a spatially uniform grid with 1,000 cells; the Maxwell molecule power-law viscosity-temperature dependence was used, $\mu \propto T$ in order to match the viscosity used in the kinetic methods.

Anisotropic Method

Kliegel [2] presents the continuity, momenta, and directional kinetic energy equations derived from a first order expansion of the Boltzmann equation for a Maxwell gas possessing the anisotropic or multi-temperature near-equilibrium velocity distribution function,

$$f_o(c) = (2\pi R)^{-3/2}(T_1T_2T_3)^{-1/2}\exp\left(-\left(\frac{{c_1}^2}{2RT_1}+\frac{{c_2}^2}{2RT_2}+\frac{{c_3}^2}{2RT_3}\right)\right), \quad (1)$$

with the mean temperature $T = (T_1+T_2+T_3)/3$. The equation set is similar to that given in [4].

Solution Method

The semi-analytic normal shock wave solution is available [3] in tabular form for a range of Mach numbers. For the numerical solution, the public domain FiPy [12] finite volume partial differential equation solver is used to integrate equations (31)-(33) of [2].

RESULTS

Normal shock structure

Figure 1 compares the calculated profiles of normalized temperature and velocity for Mach 1.2. For this relatively weak shock wave, all results are comparable, as expected. Numerical and semi-analytic solutions to the anisotropic

equations are found to be nearly identical, and only the numerical solution is presented in this figure. Note that not only macroparameters obtained by different approaches are close for this case, but also the velocity distribution functions.

Figures 2 and 3 compare the profiles for Mach 10. Under these conditions, the numerical solution of the equations of Kliegel [2] (not shown) was found to be poor. Candler *et al.* have presented results for Mach 11, finding similar issues, and suggest that retaining additional terms in the expansion could improve the robustness of the equation set. The semi-analytic solution of the equations [2] is in very good agreement with the DSMC solutions. Note also that the semi-analytic solution does predict a small, about 1%, overshoot in the mean temperature, that is typically observed in the DSMC method (see, for example, [13]). This overshoot, although somewhat larger than in DSMC, is also predicted in the solution of the ES-BGK equation. The overshoot is not seen in the solution of the BGK and the Navier-Stokes equations. As expected, the latter ones are characterized by much thinner shock than the other approaches.

It is useful to consider equation (76) of [2] for the longitudinal temperature T_1, obtained by combining the continuity and longitudinal momentum equations,

$$\frac{T_1}{T_\infty} = \frac{u_1}{u_\infty}\left[\left(1-\frac{u_1}{u_\infty}\right)\gamma M_\infty^2 + 1\right], \tag{2}$$

where γ is the gas ratio of specific heats, and the subscript ∞ indicates upstream values. Such an analytic expression for T_1 as a function of longitudinal flow velocity u_1 serves as an additional indicator of the numerical accuracy of obtained solutions.

TABLE 1. Maximum value of normalized T_1 for different approaches.

Exact	DSMC	Anisotropic Semi-analytic	Anisotropic Numerical	ES-BSK	BGK
1.3227	1.3206	1.3226	1.2579	1.3227	1.3227

This equation predicts overshoot in T_1 arises for $M_\infty > \sqrt{9/5} \sim 1.34$. A smaller (few percent) overshoot in the mean temperature also arises (see Fig. 3). As seen in Table 1, where the value of $\frac{T_1 - T_{-\infty}}{T_{+\infty} - T_{-\infty}}$ is shown at its maximum at $u_1/u_{-\infty} = 0.5$, the semi-analytical solution recovers the overshoot in temperature seen in the DSMC and ES-BGK results. Note that the DSMC value is slightly lower than the exact value given by equation 2 due to statistical scatter and a finite time step. The numerical solution of the anisotropic equations was found to underpredict the peak T_1 values, in agreement with the results of [4]; the longitudinal temperature profile obtained from (2), however, was found to yield an accurate profile. This suggests that the modifications to at least the longitudinal energy transport equation, along with more sophisticated numerical integration schemes, may be necessary to capture the strong nonequilibrium in this problem.

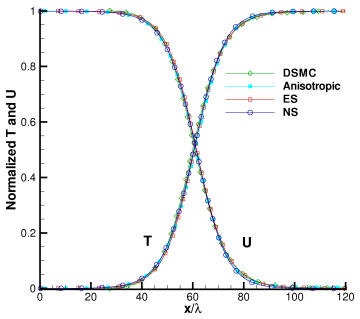

FIGURE 1. Mach 1.2 normal shock macroparameters for different numerical methods.

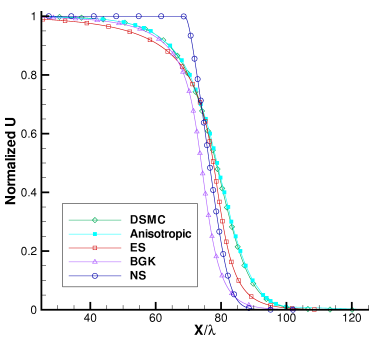

FIGURE 2. Mach 10 normal shock flow velocities for different methods.

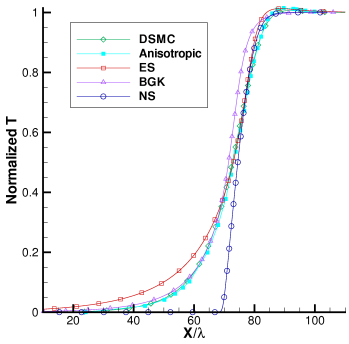

FIGURE 3. Mach 10 normal shock mean temperatures for different methods.

Figure 4 compares the directly sampled velocity distribution functions obtained from DSMC, ES-BGK, and BGK solutions at the position of maximum T_1 overshoot for the Mach 10 shock. The dotted lines show the corresponding equilibrium distribution evaluated using local macroscopic properties. Although all major macroparameters obtained by different approaches are very similar for a given value of longitudinal temperature, the distribution functions are noticeably different, especially for the BGK solution. The dissipation of the peak corresponding to the free stream flow is almost complete in the region near the maximum T_1, while for the other two approaches the distribution function is clearly bimodal. Note that similar bimodal behavior was observed for BGK upstream of the maximum T_1.

The deviation of the model distributions from the directly sampled value can be evaluated at each point through the shock and used as a measure of the relative improvement they may provide. Here, the deviation is defined as a simple density-weighted value, $\delta = \int |f_{DSMC} - f| dc_1$. Figure 5 shows the calculated profiles. In this figure, all three distribution functions are based on the macroparameters obtained from the Mach 10 DSMC computation, so they can be compared directly. For this admittedly arbitrary parameter, no model gives a clearly superior approximation to the actual DSMC distribution function. Generally, detailed comparison of distribution functions obtained by different approaches showed that the solution of the ES-BGK equation provides the best approximation to the distribution functions obtained in DSMC in terms of the shape and capturing the bimodal behavior. Note also the use of the DSMC distribution functions as the reference point is complicated by the fact that they were found to depend on the scattering law [14].

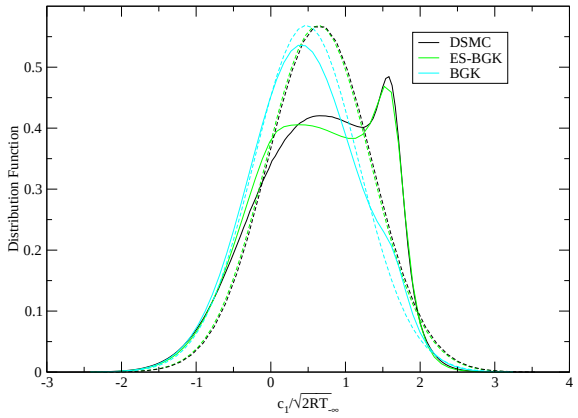

FIGURE 4. Longitudinal velocity distribution function directly sampled in DSMC, ES-BGK, and BGK, at the point where T_1 is maximum.

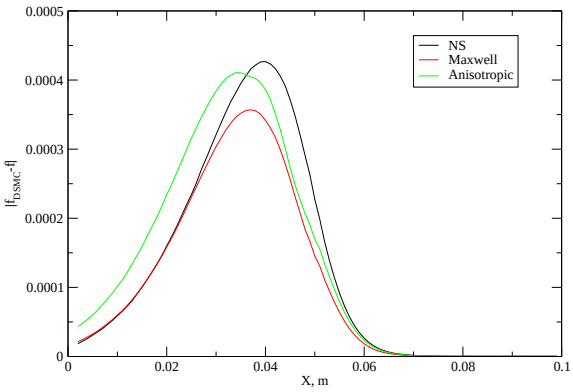

FIGURE 5. Deviation of Maxwellian, Chapman-Enskog, and anisotropic longitudinal velocity distribution functions from DSMC.

Moments of the distribution function are of more direct interest, with higher order moments providing a critical test of the relative accuracy of the models. Figure 6 shows profiles of the 4th order moment $\langle c_1^4 \rangle$ inside the Mach 10 shock, obtained by four different approaches. The semi-analytic anisotropic model agrees relatively well with the directly sampled DSMC results, generally providing noticeably better agreement than the solution of the ES-BGK equation. Interestingly, the maximum value of the 4th order moment obtained by the continuum approach (NS) is close to DSMC.

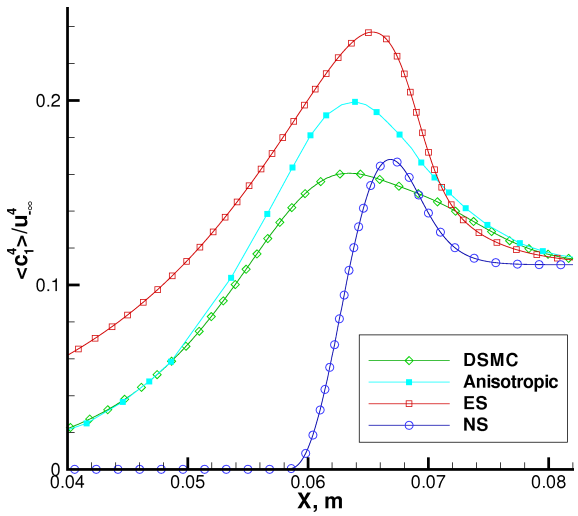

FIGURE 6. Profiles of 4th velocity moment ratio obtained with four different numerical methods.

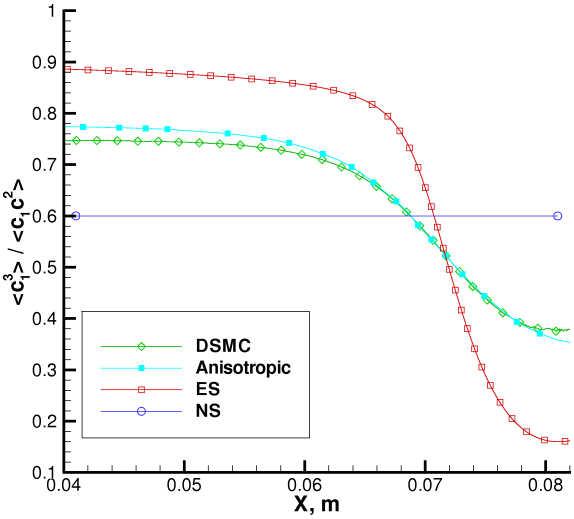

FIGURE 7. Profiles of the ratio of two 3rd order moments obtained with four different numerical methods.

An important indicator of the ability of a numerical approach to capture flow nonequilibrium is the ratio of two 3rd order moments, $\langle c_1^3 \rangle / \langle c_1 c^2 \rangle$. The numerator is the normal energy flux and the denominator is the normal total energy flux. This ratio, computed with four different approaches, is plotted in Fig. 7. Note that the near-equilibrium parts, both downstream and upstream, where the ratio becomes numerically unstable, are not shown here. The solution of the Navier-Stokes equations provides a constant value of 0.6 for this ratio, which does not depend on the location inside the shock (0.6 is in fact the equilibrium value). In the DSMC solution, the ratio varies from about 0.75 in the upstream region to about 0.38 in the downstream region. The semi-analytic anisotropic model agrees well with the DSMC results, whereas the ES-BGK solution, being qualitatively similar, noticeably overpredicts them.

Sphere cone flow

The flowfield surrounding a vehicle in hypersonic high altitude flight is a more realistic and interesting test of the applicability and accuracy of any nonequilibrium model. Here, the vehicle geometry is a 10 degree half angle cone with a spherical nosetip of radius r_n, and overall length $l = 10r_n$. The vehicle speed is $4.5 km/s$ (Mach number on the order of 15-20), and the freestream density is varied to obtain $Kn_l \sim 10^{-3}, 10^{-2}, 10^{-1}$. The property examined here is the shear stress evaluated by different approaches.

Figure 8 shows contours of the shear stress for $Kn = 10^{-3}$. The DSMC values are directly sampled $\langle c_1 c_2 \rangle$. The anisotropic values are evaluated using the DSMC macroscopic values and equation (66) of [2],

$$\tau_{12} = \frac{\rho R}{\nu} \left[T_2 \frac{\partial u_1}{\partial x_2} + T_1 \frac{\partial u_2}{\partial x_1} \right]. \tag{3}$$

The Navier-Stokes values are evaluated using

$$\tau_{12} = \mu \left[\frac{\partial u_1}{\partial x_2} + \frac{\partial u_2}{\partial x_1} \right]. \tag{4}$$

The anisotropic model reduces to this form for $T = T_i$ and using the definition of the viscosity for the Maxwell model, $\mu = \frac{\rho RT}{\nu}$.

For these near-continuum conditions, all results are comparable, as expected. The difference between shear stress values obtained with different approaches is within a few percent in the bow shock, and only slightly larger in the boundary layer. The biggest difference, up to a factor of two, is observed in the expansion region immediately after the cone rear edge. The DSMC values are lower in this region, and those obtained for the anisotropic model and NS are close.

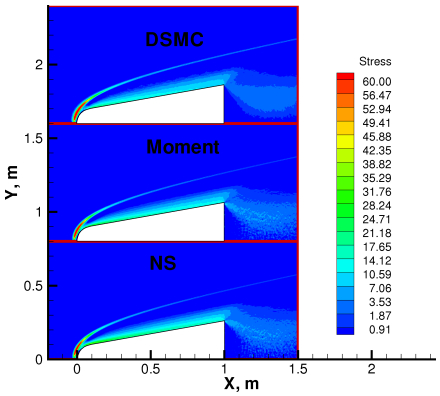

FIGURE 8. Shear stress contours, $Kn = 10^{-3}$: DSMC, Anisotropic, NS

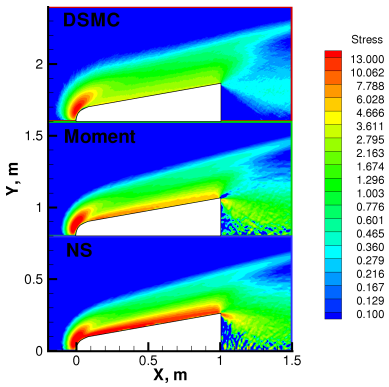

FIGURE 9. Shear stress contours, $Kn = 10^{-2}$: DSMC, Anisotropic, NS

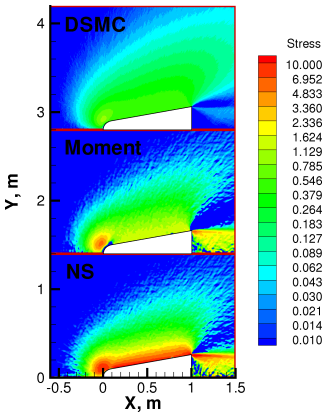

FIGURE 10. Shear stress contours, $Kn = 10^{-1}$: DSMC, Anisotropic, NS

Figure 9 shows contours of the shear stress for $Kn = 10^{-2}$. For this transitional rarefaction case, the anisotropic results show qualitative improvement relative to the NS values throughout the shock layer. Figure 10 shows contours of the shear stress for $Kn = 10^{-1}$. For this rarefied case, the anisotropic results show even a better improvement than for $Kn = 10^{-2}$ (factor of 3-5), especially in the shock region and in the boundary layer.

CONCLUSIONS

Several kinetic (the DSMC method, the solution of BGK and ES-BGK equation) and continuum (the solution of Navier-Stokes equations and the anisotropic method of Kliegel) approaches are tested in this work for their ability to accurately predict translational nonequilibrium effects. The DSMC solutions are considered benchmark, and the other approaches are compared with them on a microscopic level (velocity distribution functions) and macroscopic level (major macroparameters and higher moments). The problems under consideration are the structure of the normal shock wave, both weak and strong, and a hypersonic flow over a blunted cone.

All used numerical approaches are found to perform well, both macro and microscopically, for a Mach 1.2 shock wave, where the deviation from equilibrium is relatively small. For a Mach 10 shock, significant differences from DSMC were observed for both kinetic and continuum methods. While the solution of the ES-BGK equation provides better qualitative agreement with DSMC in terms of the longitudinal velocity distribution functions, the anisotropic model was found to perform better for both lower and higher order moments of the distribution function.

In a hypersonic flow over a blunted cone, the expression for the shear stress used in the anisotropic model are shown to offer significant improvements as compared to the conventional Navier-Stokes expression. Generally, the anisotropic equation set may be useful for flows with moderate flow nonequilibrium, and may have some potential in addressing problems associated with the transition to turbulence. For severely nonequilibrium flows, higher order terms may have to be included in the anisotropic equations. The relative importance of the assumption of Maxwell molecules used in the anisotropic equations is still to be examined.

ACKNOWLEDGMENTS

The work at USC and ERC was supported in part by the Propulsion Directorate of the Air Force Research Laboratory at Edwards Air Force Base, California. The authors wish to express their appreciation to James Kliegel for the thorough and sophisticated analysis that led to this effort, and to H. K. Cheng for sharing his vast knowledge in the field of nonequilibrium flows.

REFERENCES

1. J. C. Maxwell, *Phil. Trans. Roy. Soc.* **157**, 49–88 (1867).
2. J. Kliegel, "Maxwell Boltzmann gas dynamics," in *Rarefied Gas Dynamics*, edited by A. E. Beylich, VCH Verlagsgesellschaft mbH, Weinheim, 1991, pp. 58–66.
3. J. Kliegel, private communication (2003).
4. G. Candler, S. Nijhawan, and D. Bose, *Phys. Fluids* **6**, 3776–3786 (1994).
5. V. Dogra, J. Taylor, R. Erlandson, P. Swaminathan, and R. Nance, "Simulations of Gas Cloud Expansion Using a Multi-Temperature Gas Dynamics Model," in *Rarefied Gas Dynamics: 22nd International Symposium*, AIP Conference Proceedings, 2001, vol. 585, pp. 174–181.
6. D. Baganoff, *Phys. Fluids* **14**, 3403–3413 (2002).
7. M. Ivanov, G. Markelov, and S. Gimelshein, Statistical simulation of reactive rarefied flows: numerical approach and applications (1998).
8. *FLUENT 6.1 User's Guide*, Fluent Inc. (2003).
9. M. Ivanov, and S. Rogasinsky, *Soviet J. Numer. Anal. Math. Modeling* **3**, 453–465 (1988).
10. G. Bird, *Molecular Gas Dynamics and the Direct Simulation of Gas Flows*, Clarendon Press, Oxford, 1994.
11. L. Mieussens, *J. Comp. Physics* **162**, 429–466 (2000).
12. D. Wheeler, J. Guyer, and J. A. Warren, *FiPy User's Guide* (2007).
13. G. Bird, "Perception of numerical methods in rarefied gas dynamics," in *Rarefied Gas Dynamics*, edited by E. Muntz, D. Weaver, and D. Campbell, American Intstitute of Aeronautics and Astronautics, Washington, D.C., 1989, vol. 118, pp. 211–226.
14. S. Gimelshein, M. Ivanov, and S. Rogasinsky, "Investigation of shock wave structure by majorant cell and free cell schemes of DSMC," in *Rarefied Gas Dynamics*, edited by A. E. Beylich, VCH Verlagsgesellschaft mbH, Weinheim, 1991, pp. 718–726.